

## APPENDIX C

### *Sediment Transport Scaling for Physical Models*

*Clifford A. Pugh*

#### C.1 INTRODUCTION

Reclamation experience with sediment models started in the early 1950s. Several predesign models were developed for the Missouri River Basin and Middle Rio Grande diversions. The sediment used for all these studies was a fine uniform sand with a mean diameter of 0.2 mm. It was recognized that settling velocity is very important in determining when a particle will remain at rest or how far it will travel once lifted into the flow. The 10% model sizes were scaled by settling velocity according to the Froude law, that is, by the square root of the length ratio (not by the geometric scale ratio).

These models were force fed with sediment to develop bed slopes sufficient to move sediment at rates estimated by theoretical sediment bedload equations. Bed slopes that were developed in this manner were generally exaggerated because of friction differences between model and prototype. However, at diversions, flow splits occur within a short reach in the direction of flow, and the structure does not need to be distorted.

Sediment concentration was measured in all the component flows of the models. Concentration ratios of the measured delivery rate to the river concentration were used to compare the relative amount of sediment in the delivery for different trial diversion arrangements (Carlson 1970).

#### C.2 MODELING CONSIDERATIONS

##### C.2.1 Similitude

Hydraulic models are used because of the large number of variables involved and because of complicated boundary conditions. Hydraulic models may be either true or distorted models. True models have all of the significant characteristics of the prototype reproduced to scale (geometrically similar) and satisfy model design restrictions (kinematic and dynamic similitude). Model-prototype comparisons have

shown that correspondence of behavior is often well beyond expectations, as has been attested by the successful operation of many structures designed from model tests.

A model and prototype are designed to be similar geometrically, kinematically, and dynamically. Geometric similarity exists when the ratios of all homologous dimensions between model and prototype are the same. The geometric scale ratio, or length ratio, is denoted by  $L_r$  which is the ratio  $L_m/L_p$ , where the subscripts  $m$  and  $p$  refer to the model and prototype, respectively. Kinematic similarity, or similarity of motion, implies that the ratios of velocities and accelerations between model and prototype are equal. Dynamic similarity requires that the ratios of homologous forces between the model and prototype be the same. Possible hydraulic forces are caused by gravity, viscosity, pressure, surface tension, and elasticity.

For hydraulic modeling, the more important, dimensionless parameters are dimensionless ratios formed with respect to inertia.

The Reynolds number is the ratio of inertia and viscous forces:

$$R = \frac{VD}{\nu} \quad (C-1)$$

An open-channel model is normally operated according to the ratio of inertia and gravity forces. This ratio is represented by the Froude number:

$$F = \frac{V}{\sqrt{gD}} \quad (C-2)$$

The scale relationships for open-channel flow based on Froude scaling follow:

$$\text{Length} = L_r \text{ (geometric scaling)}$$

$$\text{Area} = L_r^2$$

$$\text{Volume} = L_r^3$$

$$\text{Time} = L_r^{1/2}$$

$$\begin{aligned}\text{Force} &= L_r^3 \\ \text{Shear} &= L_r \\ \text{Velocity} &= L_r^{1/2} \\ \text{Discharge} &= L_r^{5/2}\end{aligned}$$

### C.2.2 Similitude Deficiency of Froude Scaling

The tractive stress on a particle fluctuates because of turbulence. The drag force and turbulence are a function of viscous forces (Reynolds number). Vanoni (1975) discussed the important variables involved in the present knowledge of sediment transport in a section on "Fundamentals of Sediment Transport" in the *Sedimentation Engineering* handbook. He reduced the sediment discharge rate ( $Q_s$ ) to the following relationship (these symbols are defined in the glossary):

$$Q_s = f(Q, R, d, v, \rho, \sigma, \sigma_s, q, w, g) \quad (\text{C-3})$$

### C.2.3 Tractive Stress

Models involving erosion of noncohesive bed material must simulate tractive stress ( $\tau_0$ ), because the tractive stress causes the drag force required to overcome the gravity forces holding a particle in place (See Fig. C-1).

Froude scale models do not necessarily simulate the tractive forces and sediment erosion accurately because Froude

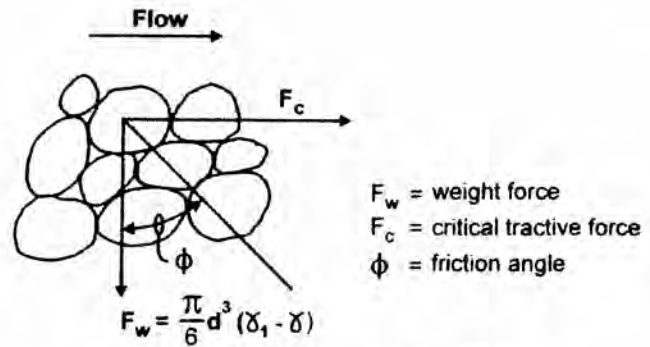


Fig. C-1. Forces holding sand grains in place.

scaling does not simulate viscous forces. However, sediment sizes can be adjusted (distorted) in some Froude scale models to compensate for a Reynolds number that is too low. The Reynolds number offset ratio ( $R_r$ ) of a Froude scale model can be determined by substituting the Froude scaled variables (velocity and length) into Eq. (C-1) for the Reynolds number (Pugh and Dodge 1991), resulting in

$$R_r = L_r^{3/2} \quad (\text{C-4})$$

This means that a 1/10 scale model would have a Reynolds number ratio ( $R_r$ ) of

$$(1/10)^{3/2} = 1/31.6$$

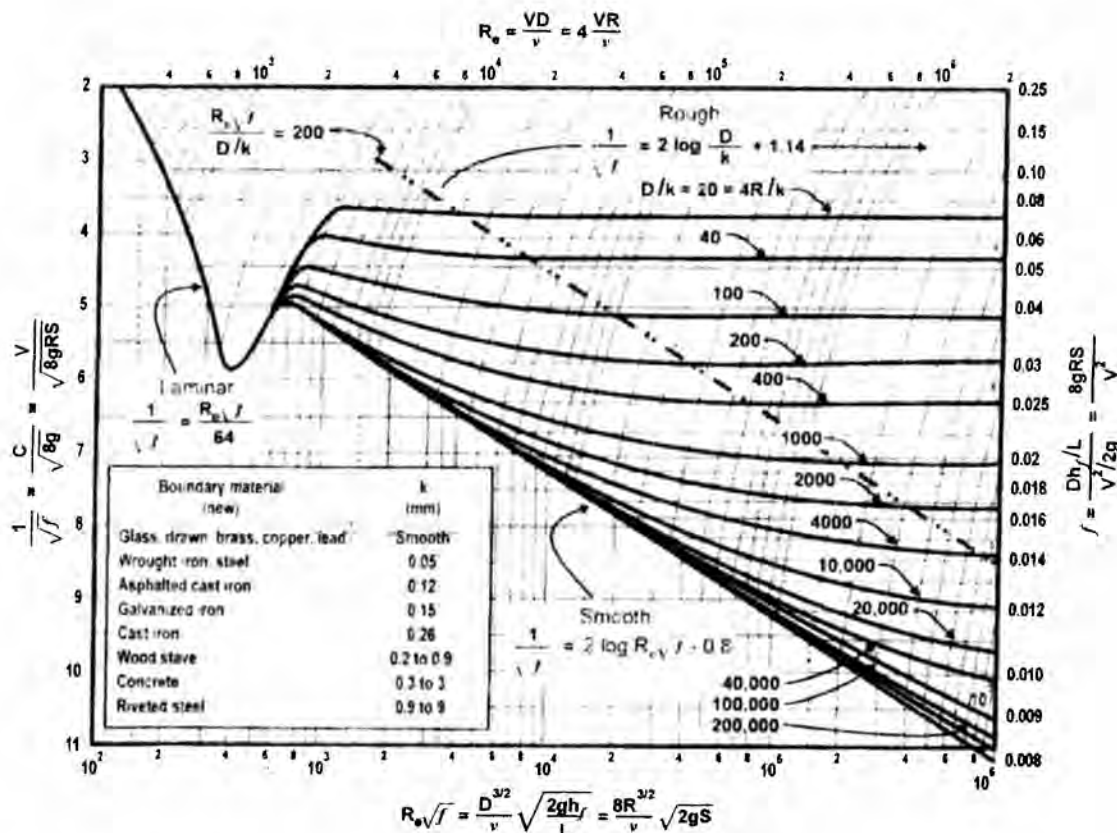


Fig. C-2. General resistance diagram for uniform pipe flow.

Therefore, if the prototype Reynolds number is, say,  $3 \times 10^6$ , the model Reynolds number for a Froude scaled model would be  $9.5 \times 10^5$ . If we refer to the Darcy-Weisbach friction diagram (See Fig. C-2) for an arbitrary relative roughness ( $4R/k$ ) of 10,000 (Rouse 1948), the model friction factor ( $f$ ) would be 0.0135 in the model and 0.0125 in the prototype. This indicates that the model should be designed to be smoother than geometrically scaled roughness (Kobus 1980) (or distorted to a steeper slope) to compensate for the relatively greater influence of viscous forces in the model.

#### C.2.4 Structural Modeling of Cohesive Sediment

If erosion of cohesive sediment occurs by chunking action such as cutback scour, or in a controlled manner, such as by the erosion of an impervious cohesive core in a fuse plug (Figs. C-3 and C-4), the model needs to include the effects of elastic forces of the cohesive sediment as well as of gravity (Pugh 1985). The ratio of the gravity and elastic forces results in the structural integrity number ( $M$ ), expressed as

$$M = \gamma \cdot L / E \quad (C-5)$$

where  $E$  is the modulus of elasticity of the cohesive sediment material, and  $L$  is a characteristic length.  $M$  must be the same in the model and the prototype.

In the fuse plug model it was difficult to find an impervious material with the proper modulus of elasticity to satisfy Eq. (C-5), so the core was analyzed as a structural slab, with pieces breaking off due to the weight of sand and water above as the cohesionless material in the pilot channel and in the main shell during the lateral erosion process eroded downstream from the core. The clay portion was reduced in thickness to adjust the moment of inertia, to compensate for the relatively high  $E$  of the model core. This method was successful, since it qualitatively simulated the observed behavior of pilot channel erosion in prototype tests, such as the Oxbow experiment (Albrook 1959).

#### C.2.5 Shields Diagram

Shields developed a diagram (Fig. 2-18) relating dimensionless shear stress ( $\tau^*$ ) to a boundary or grain Reynolds number ( $R$ ). Shields used this diagram to define critical shear stress ( $\tau_c$ ) (the stress required for incipient motion of noncohesive sediment). This concept has been expanded by others (Fig. C-5) to include dimensionless unit sediment discharge ( $q_s^*$ ), where

$$q_s^* = \frac{q_s}{u_*^* d} \quad (C-6)$$

#### C.2.6 Dimensionless Unit Sediment Discharge

Dimensionless unit sediment discharge should be the same in the model and the prototype to properly simulate sediment transport. The following procedure explains how to compute adjustments in model sediment size and/or weight, in order to compensate for a relatively low Reynolds number in a Froude-scaled model. These corrections should yield a near-uniform  $q_s^*$  in the model and the prototype.

Vanoni (1975) used Taylor's data to show that dimensionless unit sediment discharge at low transport levels falls very close to the Shields curve for incipient motion (Fig. C-5). To properly simulate sediment transport, the dimensionless unit sediment discharge rate ( $q_s^*$ ) must be approximately the same in the model and the prototype.

For a model with a grain Reynolds number ( $R^*$ ) greater than about 5 and less than 100, the unit sediment discharge rate for the model would be higher than that for the prototype (if the model sand grains are sized according to geometric scaling) because the dimensionless shear stress ( $\tau^*$ ) is about the same in the model and the prototype.

For grain Reynolds number

$$R^* = \frac{u_*^* d}{\nu} \quad (C-7)$$

and dimensionless shear stress

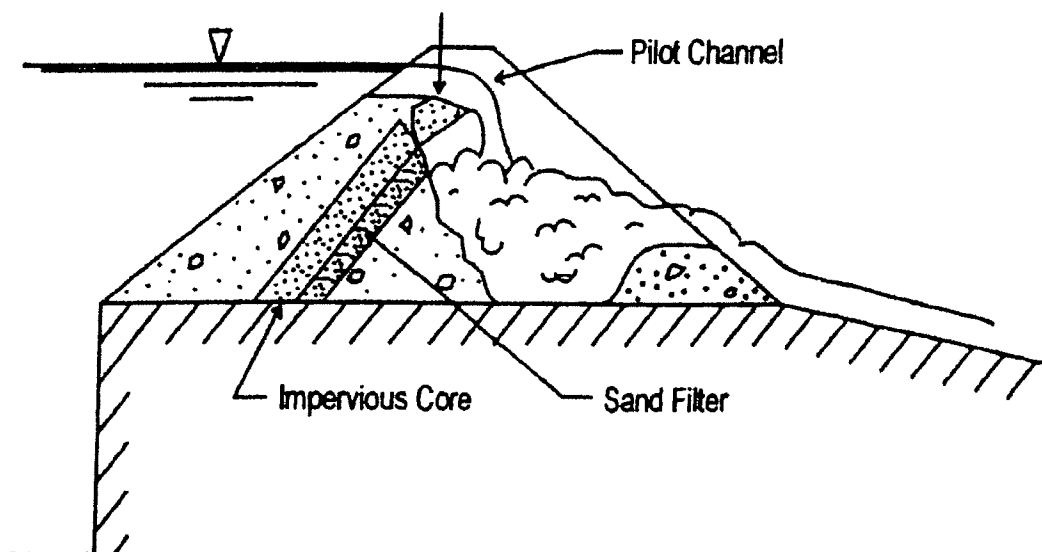


Fig. C-3. Structural modeling of fuse plug core.

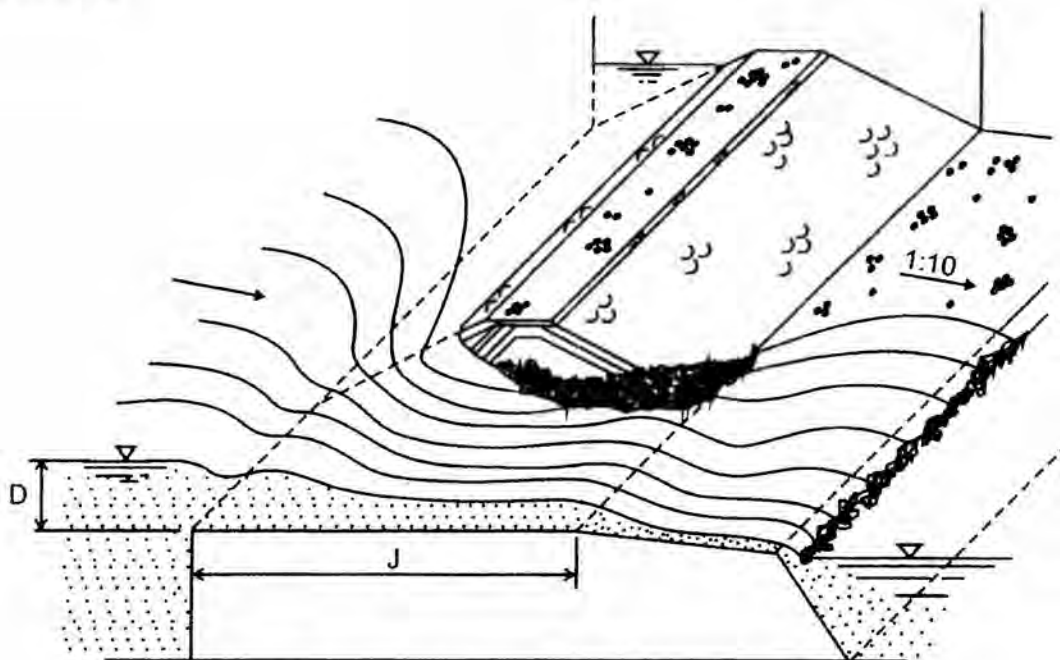


Fig. C-4. Fuse plug lateral erosion process.

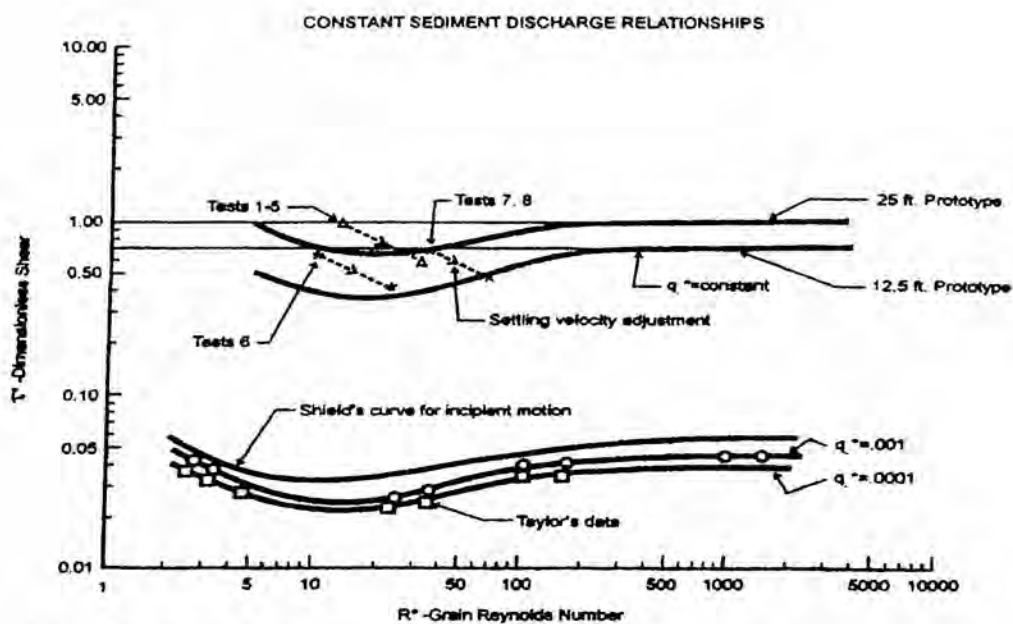


Fig. C-5. Shields diagram, dimensionless unit sediment discharge curve ( $q^*$ ), versus dimensionless shear stress ( $\tau^*$ ) and grain Reynolds number ( $R^*$ ). Effects of settling velocity adjustments are shown.

$$\tau^* = \frac{\tau_o}{(\gamma_s - \gamma)d} \quad (C-8)$$

it can be shown that dimensionless shear stress is a form of the Froude number, the submerged specific gravity of the sediment and the ratio between the flow depth and the particle diameter.

The shear velocity is

$$u^* = \sqrt{\frac{\tau_o}{\rho}} \quad (C-9)$$

Therefore the tractive shear stress is,

$$\tau_o = \rho \cdot u^{*2} \quad (C-10)$$

and the unit force (or weight) is

$$\gamma = \rho \cdot g \quad (C-11)$$

Substituting equation (C-11) into Eq. (C-10):

$$\tau_o = \left[ \frac{\gamma \cdot u^{*2}}{g} \right] \quad (C-12)$$

Substituting Eq. (C-12) into Eq. (C-8):

$$\tau^* = \left( \frac{u^{*2}}{gd} \right) \cdot \left( \frac{\gamma}{\gamma_s - \gamma} \right) \quad (C-13)$$

The first term in Eq. (C-13) is in the form of a Froude number; the second term is the ratio of the densities of the water and the sediment, when gravity is factored out.

It is sometimes more convenient to compute  $\tau^*$  using a form of Eq. (C-13) relating to the Darcy-Weisbach friction factor ( $f$ ). Rouse (1948) has shown that the shear velocity is a function of the water velocity ( $V$ ) and the friction factor ( $f$ ),

$$u^* = \sqrt{gRS} = \sqrt{\frac{\tau_o}{\rho}} = V \cdot \sqrt{\frac{f}{8}} \quad (C-14)$$

Substituting Eq. (C-14) into Eq. (C-13),

$$\tau^* = \left( \frac{V^2 f}{8gd} \right) \cdot \left( \frac{\gamma}{\gamma_s - \gamma} \right) \quad (C-15)$$

To determine  $f$  in an open channel, the Reynolds number ( $R$ ) is computed according to the equation (Rouse 1948)

$$R = 4R \cdot V/\nu \quad (C-16)$$

where  $R$  = the hydraulic radius and  $\nu$  is the kinematic viscosity. The relative roughness (needed to determine  $f$ ) is defined as

$$\text{relative roughness} = \frac{K_s}{4 \cdot R} \quad (C-17)$$

where

$K_s$  = roughness height.

Kamphuis (1974) found that

$$K_s = 2 \cdot d_{90} \quad (C-18)$$

where

$d_{90}$  = the particle diameter at which 90% of the grains are smaller in diameter.

The hydraulic radius ( $R$ ) can be taken as the flow depth, if the channel is relatively wide.

If a model is scaled geometrically according to Froude scaling ( $\tau_m^* = \tau_p^*$ ), the model unit sediment discharge rate ( $q_s^*$ ) will be too great in the range  $5 < R^* < 100$ . Therefore, the model sediment should be adjusted to properly simulate sediment transport in this range. A diagram of settling velocity ( $w$ ) of sand and silt particles in water (Fig. C-6) illustrates that small particles (<1 mm in diameter) settle at progressively lower velocities as the particles become smaller. For particle diameters larger than 1 mm, the settling velocity is a function of the particle diameter ( $d$ ) to the 1/2 power. This is consistent with Froude model scaling for velocity,  $V_r = L_r^{1/2}$ .

### C.2.7 Settling Velocity Adjustment

By increasing the size of a model sediment grain, the settling velocity can be corrected to the proper value for Froude scaling in the model for a grain Reynolds number in the range  $5 < R^* < 100$ . For example, according to geometric scaling, a 1:10 scale model of prototype sand 2.0 mm in diameter would use sand 0.2 mm in diameter. However, the settling velocity would then be about 0.02 m/s (see Fig. C-6), when it should be 0.049 m/s, according to Froude scaling. If the model particle diameter is adjusted from 0.2-mm to 0.4-mm, the settling velocity is corrected to 0.049 m/s, the proper value for Froude scaling. Fig. C-7 gives sample sediment size adjustments for a fuse plug prototype gradation curve of the sand and gravel zone of the embankment (1:10 and 1:25 scale models). Note that the model gradation curves are closer to geometric scaling in the larger sizes. After the model gradation is determined, the test material may need to be created by mixing uniform-sized sands, or an available natural sand gradation may be close enough to the design gradation to suit the purpose.

The effect of settling velocity adjustment on the dimensionless sediment discharge rate ( $q_s^*$ ) is shown in the examples for fuse plug model scaling plotted in Fig. C-5. Note that the model values of dimensionless shear ( $\tau^*$ ) for geometrically scaled particles, before settling velocity adjustments, are about the same as the prototype values they simulate (Froude scaling). Tests 1 to 5 simulate a 7.6-m (25-ft)-high prototype fuse plug embankment, and tests 6, 7, and 8 simulate a 3.8-m (12.5-ft)-high prototype embankment. However, the value of  $q_s^*$  must be the same in the model and prototype to properly

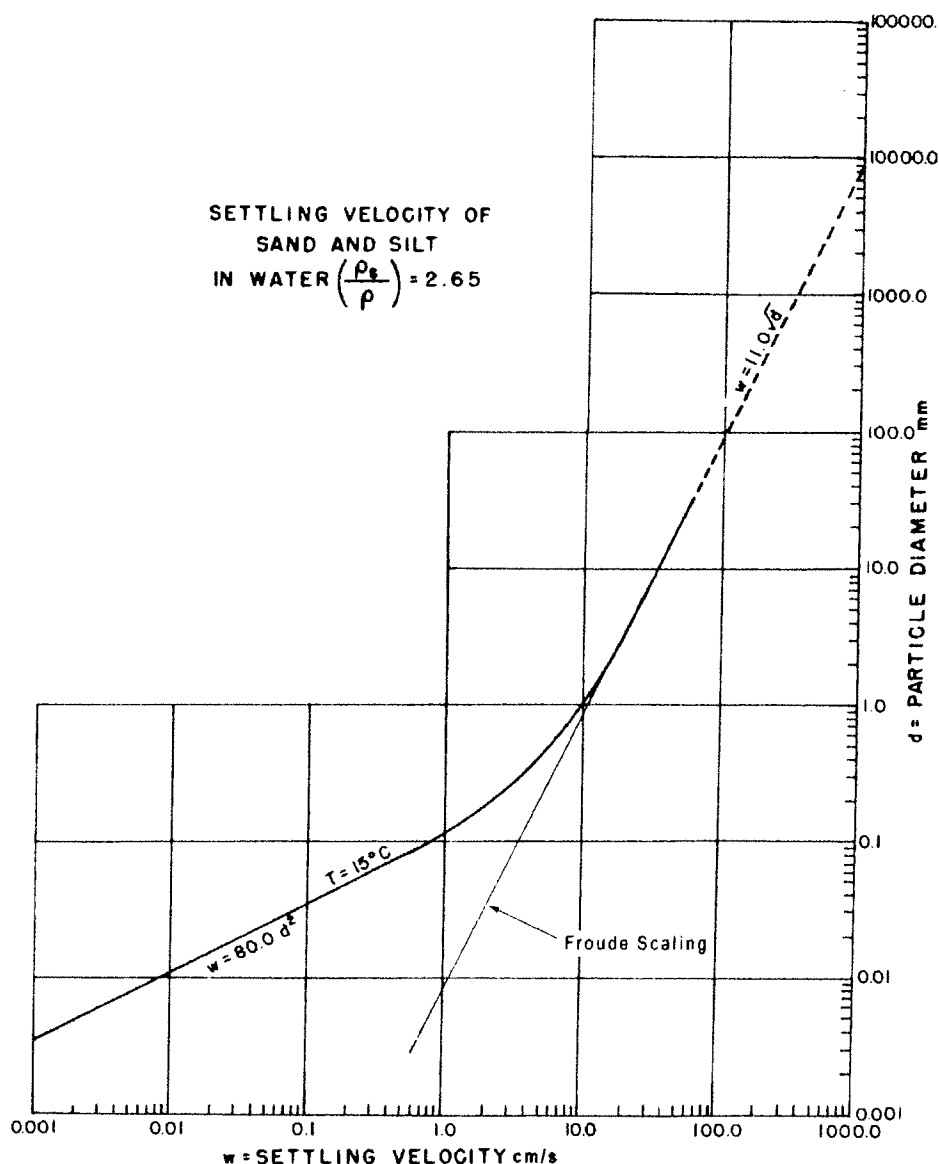


Fig. C-6. Settling velocity of sand and silt in 15° C water.

scale the time rate of sediment transport. When the model grain sizes are adjusted for settling velocity (as described above), the value of  $\tau^*$  decreases, whereas, the value of  $R^*$  increases (see the effect of the change in Fig. C-5). This adjustment brings the model value of  $q_s^*$  much closer to the estimated prototype curves for  $q_s^*$ . The method applies to noncohesive materials in the model and in the prototype, and must be checked for various ranges of grain sizes, locations, and model flow conditions. If model Reynolds number is less than 5, a lighter sediment weight is often substituted to approximate the proper model sediment transport rate. If the model  $d$  is greater than 1mm, no adjustment in sediment grain size is generally necessary. However, keep in mind that the model  $R^*$  values will be lower in certain zones in the model, so each area of interest to sediment transport in the model needs to be evaluated to properly simulate sediment-transport scaling. For instance, sediment is

sometimes drawn back into stilling basins by surging reverse currents at the end of energy-dissipation-type stilling basins. To simulate this movement in a physical model, the velocities should be measured and the procedure described above should be applied to determine the appropriate model sediment size and weight to simulate transport in this area.

It is desirable to make the model scale as close as possible to the prototype so that scale effects are minimized. This is why model sediment is sometimes simulated with a lightweight material, such as coal dust, in a model with a relatively small scale,  $R^* < 5$ .

### C.2.8 Model-Prototype Comparison

Photographs of the laboratory fuse plug tests are shown in Figs. C-8 and C-9. The lateral erosion process after the initial

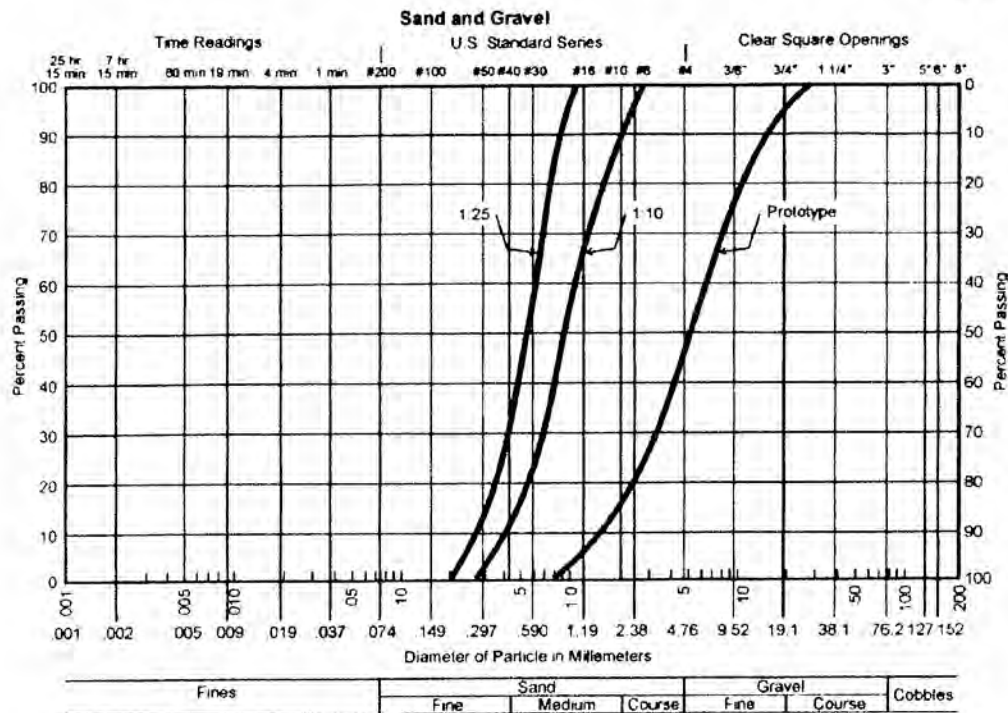


Fig. C-7. Sample sediment size adjustments for fuse plug prototype gradation curves. Main sand and gravel shell (1:10 and 1:25 scale models).



Fig. C-8. Fuse plug test; lateral erosion in progress, initial breach is complete.

breach is shown in Fig. C-8. The rate of erosion is controlled by the embankment geometry and the material gradation and placement of the zoned embankment.

The erosion rate of the main 'shell,' downstream from the inclined impervious core, controls the lateral erosion rate. This zone (sand and gravel) was carefully modeled with the gradations shown in Fig. C-7. The gradations were obtained by mixing proportions of uniform-sized sands to

reconstruct the gradation curve determined by the scaling process described above. After the scaled gradations were mixed, they were tested with sieve analysis to confirm the proper gradation. The material was placed in lifts and compacted to 70% relative density by weighing and compacting each lift in the model. The gradation and compaction of the graded material are important in properly simulating the erosion rate.

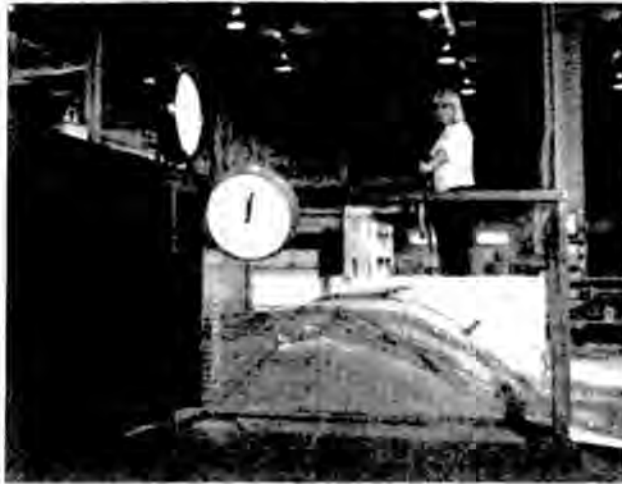


Fig. C-9. Fuse plug model test at Reclamation's hydraulic laboratory; pilot channel breach.

Figure C-9 shows the initial breach process in the pilot channel section. This process is controlled by the structural strength of the cantilevered core, as described above. The erosion of the shell material beneath the core controls the initial breach rate of the pilot channel, as well as the lateral erosion process after the initial breach. During the initial breach and the lateral erosion, the upstream water surface was maintained constant to approximate a prototype condition with much more reservoir storage. This also eliminates the variable water surface as a complicating variable in the tests.

A field test was performed in 1959 (Albrook 1959) on a 1:2 scale model of the 8.2-m-high fuse plug used for the Oxbow Project on the Snake River in Idaho. The gradation curve for the 4.1-m-high test embankment was very close to the prototype gradation simulated in the fuse plug model study conducted at the Bureau of Reclamation's hydraulic laboratory in 1985.

The geometrically scaled sand grain diameters in the model were adjusted in size with the settling velocity adjustment correcting for the Reynolds number offset (Pugh 1985).

The lateral erosion rate predicted by Reclamation's 1:10 scale model for the Oxbow field test was 1.66 m/min as compared to 1.71 m/min measured during the Oxbow test (Fig. C-10). The difference of 2% is well within experimental accuracy and seems to substantiate the scaling technique.

### C.3 Nomenclature

Subscripts  $m$  and  $p$  refer to the model and prototype, and  $r$  refers to the ratio between the model and prototype.

$D$  = water depth; pipe diameter in Fig. C-2

$d$  = sand grain diameter

$d_{90}$  = grain diameter at which 90% of the grains are smaller

$E$  = modulus of elasticity of the cohesive sediment material

$F = V/\sqrt{gD}$  = Froude number

$F_c$  = critical tractive force

$F_w$  = weight force

$f$  = the Darcy-Weisbach friction factor

$g$  = acceleration due to gravity

$K_s = 2 \cdot d_{90}$  (rugosity)

$L$  = a characteristic length

$L_r$  = length ratio between model and prototype

$M$  = the structural merit number

$Q_s$  = sediment discharge rate

$q$  = unit discharge

$q_s$  = unit sediment discharge

$q_s^*$  = dimensionless unit sediment discharge

$R$  = the hydraulic radius

$R = Vd/\nu$  = Reynolds number

$R' = u^* \cdot d/\nu$  = boundary or grain Reynolds number

$R_r = L_r^{1/2}$  = Reynolds number offset ratio for a Froude-scaled model

$S$  = water surface slope

$u^*$  = shear velocity

$V$  = average water velocity at any point

$w$  = settling velocity of sand and silt in water

$\gamma$  = specific weight of water

$\gamma_s$  = specific weight of sediment

$\rho$  = water density

$\rho_s$  = sediment density

$\sigma$  = surface tension

$\sigma_s$  = standard deviation of grain sizes

$\tau^*$  = dimensionless shear stress

$\tau_o$  = the tractive stress

$\tau_c$  = critical shear stress, where sediment starts to move

$\nu$  = the kinematic viscosity

$\phi$  = sediment friction angle

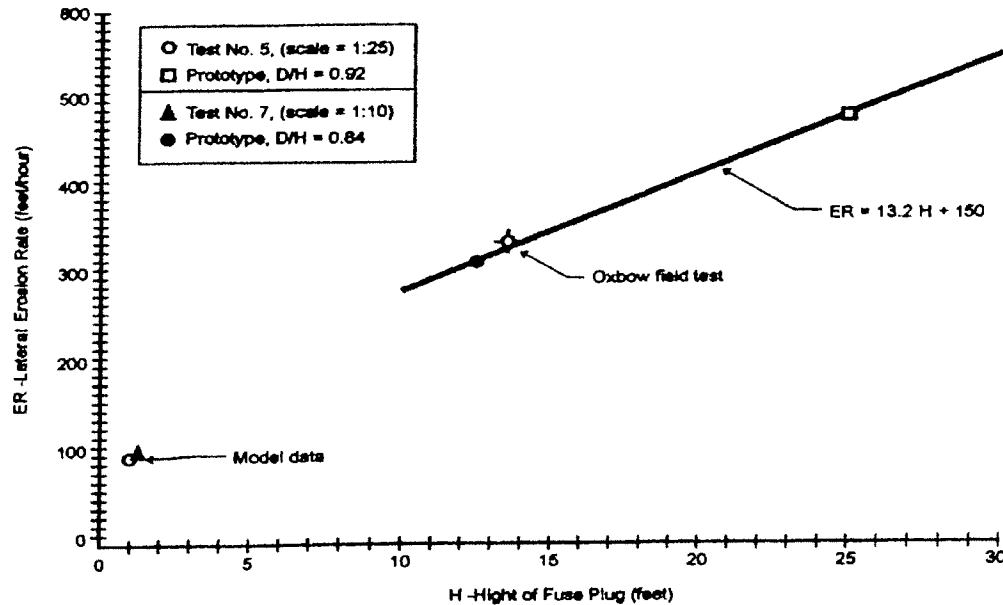


Fig. C-10. U. S. Bureau of Reclamation fuse plug model test results (Oxbow field test included).

## REFERENCES

- R. L. Albrook Hydraulic Laboratory and International Engineering Company, Inc., (Albrook). (1959). *Oxbow hydroelectric development, Idaho spillway with fuse plug control, model studies of fuse plug washout*, Washington State College, Pullman, Wash.
- Carlson, E. J. (1970). "Laboratory and field investigations of sediment control structures at diversion dams." International Commission on Irrigation and Drainage, Ninth Congress.
- Kamphuis, J. W. (1974). "Determination of sand roughness for fixed beds." *Journal of Hydraulic Research* 12(2), 193-203.
- Kobus, H. (1980). "Hydraulic Modeling." *Bulletin 7*, German Association for Water Resources and Land Improvement, Verlag Paul Parey, Hamburg, Germany.
- Pugh, C. A. (1985). "Hydraulic model studies of fuse plug embankments." *REC-ERC-85-7*, U.S. Bureau of Reclamation, Denver, Colo.
- Pugh, C. A., and Dodge, R. A. (1991). "Design of sediment models," Fifth Federal Interagency Sedimentation Conference.
- Rouse, H. (1948) *Elementary mechanics of fluids*. Wiley, London, 201-203.
- Vanoni, Vito A. (1975). "Sedimentation engineering." *Manual No. 54*, ASCE Task Committee for Preparation of the Manual on Sedimentation of the Sedimentation Committee of the Hydraulics Division, ASCE, New York.